MAGIC-TDAS 01-03
R. Böck,
H. Kornmayer,
W. Wittek

Outline of a standard analysis for MAGIC (including Monte Carlo work)

R. Böck, H. Kornmayer, W. Wittek
Rudolf.Bock@cern.ch, h.kornmayer@web.de, wittek@mppmu.mpg.de

17th September 2001

Abstract

Contents

1 Aim of this paper

The aim of this paper is to describe the procedure to obtain the absolute energy spectrum of a point source from the data taken with MAGIC. This includes work on Mont Carlo (MC) data and the analysis of real data.

Various steps in the procedure will depend on details of the MC generation, on the way the real data are taken, etc.. These details have therefore to be specified, which is done in Section 2.

In Section 3 some basic definitions and formulas are collected in order to avoid any misunderstanding of the meaning of frequently used terms.

Section 4 describes the MC work and Section 5 the actual analysis of the real data.

One aim of this paper is also to define jobs for those who want to join the activities in the software developments. As will be seen, some ingredients both for the MC work and the real data analysis are available. However, many parts have yet to be implemented, others have to be changed, modified, improved or extended. Last not least extensive tests have to be performed.

2 Assumptions

The assumptions for a 'standard analysis' listed below are the result of discussions in the software group. Some of them are rather arbitrary. They should by no means be understood as final or optimal choices. They should be considered as a starting point. As our experience with the analysis grows we may have to revise some of the assumptions.

The aim in all what follows is to define a strategy that is as simple and as robust as possible. Tests that have yet to be performed will tell us whether the assumptions are reasonable and realistic.

The assumptions are :

2.1 Mode of observation

Data are taken in the wobble mode ([4]). This means that the telescope is directed not to the position of the selected source but rather to a position which has a certain offset ($\Delta\beta$) from the source position. Every 20 minutes of observation the sign of $\Delta\beta$ is changed. The two wobble positions are called wobble position 1 and 2.

$\Delta\beta$ may be chosen to be a direction difference in celestial coordinates (declination δ, right ascension Φ), in local coordinates (zenith angle Θ, azimuthal angle ϕ) or in coordinates in the camera system. However the direction $\Delta\beta$ is defined, the sky region projected onto the camera is different for wobble positions 1 and 2.

If $\Delta\beta$ is defined to be a direction difference in celestial coordinates, the sky region projected onto the camera for a fixed wobble position remains the same during tracking of a source, although the sky image is rotating in the camera (see [5]).

If $\Delta\beta$ is defined to be a direction difference in local coordinates, the sky region projected onto the camera is changing continuously during tracking of a source. The centers of the projected sky regions lie on a circle, which is centered at the source position.

$\Delta\beta$ may be defined to be a direction difference along the horizontal axis of the camera, in which case (for a fixed wobble position) the source would appear always at the same position (on the x-axis) in the camera. This choice has the advantage that the 'anti' source position (the position in the camera obtained by reflecting the source position at the camera origin) is in many respects equivalent to the source position. In particular, the 'anti' source position has the same zenith angle as the source position. The 'anti' source position is therefore very well suited for estimating the background near the source position (see below). Here 'background' means the diffuse hadronic background and the diffuse electron background.

We propose this type of wobbling with $\Delta\beta = 0.4°$. Note that the outer radius of the outer part of the camera is $2°$, the radius of the inner part is $1.25°$ and the radius of the trigger region is $0.8°$. For very small Θ ($\Theta < 1°$) $\Delta\beta$ has to be defined differently, for example along the vertical axis of the camera system. Details about this wobble mode are given in a separate report [13].

The wobble mode has to be understood as an alternative to taking on- and off-data in separate runs. Choosing the wobble mode thus implies that one is taking on-data only, from which also the 'off-data' have to be obtained by some procedure.

2.2 Pedestals

Pedestals and their fluctuations are initially not determined from triggered showers but rather from pedestal events. The pedestal events are taken 'continuously' at a constant rate (of say 5 Hz), in addition to pedestal runs at the beginning and at the end of a data taking run. In this way the pedestals and their fluctuations are always up to date, and the presence of stars and their position in the camera can be monitored continuously.

2.3 Data analysis

In the most general case the data analysis has to take into account

a) the direction (Θ, ϕ) the telescope is pointing to

b) the position of the source in the camera (i.e the wobble position)

c) the sky region projected onto the camera, which depends on the time of observation

d) the orientation of this sky region in the camera, which depends on the time of observation

e) the presence of moon light

e) the special trigger conditions

Because c), d) and e) depend on the source being observed, this would imply separate analysis procedures for the individual sources. The aim is to develop an analysis chain, which is applicable to all sources simultaneously. This may be achieved by trying to describe

- the level of the light of the night sky (LONS) and the presence of moon light by the pedestal fluctuations, averaged over all pixels,
- and the presence of stars in the field of view of the camera by the pedestal fluctuations in individual pixels.

With moon light it will be necessary to run the detector in special modes, like choosing different PM-HV settings.

The aim is thus an analysis which depends on

- The telescope orientation (Θ, ϕ)
- The position of the source in the camera (wobble position)
- The pedestal fluctuations
- THE PM-HV settings

These dependencies have to be taken into account for

a) the γ/(hadron+electron) separation cuts

b) the 'standard cuts' which define the 'standard samples' of γs and hadrons respectively

c) the effective collection areas for the standard γ and hadron samples respectively

The γ/(hadron+electron) separation cuts and the 'standard cuts' are usually given in terms of cuts on the image parameters or on variables derived from them. These cuts will depend on (Θ, ϕ), the pedestal fluctuations and the PM-HV settings. Of course, one could also try to redefine the image parameters using the pedestal fluctuations and PM-HV settings, such that the cuts on the redefined image parameters no longer depend explicitely on the pedestal fluctuations and PM-HV settings. Approaches in this direction were followed in some analyses of HEGRA telescope data [7].

The main parameter of the telescope orientation is the zenith angle Θ. It has to be investigated whether also the azimuthal angle ϕ has to be taken into account, for example because of influences from the geomagnetic field (see [10]).

2.4 Trigger conditions

The basics of the MAGIC trigger are explained in [6]. For the level-1 trigger conditions we propose as a starting point [14] :

- Discriminator threshold at 3-4 mV (see Fig.3 of [14]), gate length 6 ns.
- Four closed-pack neighbour pixels. This means that there should be at least 4 fired pixels which are neighbours, such that if one of them is removed the remaining 3 pixels are still neighbours.
- Minimum overlapping/coincidence time 0.25 ns.
- Suppression of triggering on stars : ignore pixels which have more than 0.5 photoelectrons per ns at a discriminator threshold of 7 mV (see [14]).

2.5 Standard selections

The criteria for the 'standard' γ and hadron samples have to be clearly defined. Perhaps in the analysis program a special class should be defined in which everything dealing with the 'standard selections' is collected. Monte Carlo work on triggered events is needed to get initial settings for the standard selection criteria.

3 Definitions and formulas

3.1 Definitions

- The direction (Θ, ϕ) :
  (Θ, ϕ) denotes the direction the telescope is pointing to, not the position of the source being observed.

- Image parameters :
  The standard definition of the image parameters is assumed. See for example [1, 2, 3]. We should also make use of additional parameters like asymmetry parameters, number of islands or mountains etc.

Quantities which are not directly measurable, but which can be estimated from the image parameters are :

- The impact parameter :
  The impact parameter p is defined as the vertical distance of the telescope from the shower axis.

- The energy of the shower

3.2 Formulas

a) Differential gamma flux of a point source

The differential gamma flux from a point source s is given by

$$\Phi_s^\gamma(E) \;=\; \frac{dN_s^\gamma}{dE \cdot dF \cdot dt} \tag{1}$$

where dN_s^γ is the number of gammas from the source s in the bin dE, dF, dt of energy, area and time respectively. dF is an area perpendicular to the source direction. For infinitesimal dE, dF, dt the number of true γs is thus

$$dN_s^{\gamma,true}(E,\Theta,F) \;=\; \Phi_s^\gamma(E) \cdot dE \cdot dF \cdot dt \tag{2}$$

We denote the probability for 'observing' a gamma shower with energy E, zenith angle Θ and position F in a plane perpendicular to the source direction by $R^\gamma(E,\Theta,F)$. Depending on the special study, the term 'observing' may mean triggering, reconstructing, etc.
The effective collection area is defined as

$$F_{eff}^\gamma(E,\Theta) \;=\; \int R^\gamma(E,\Theta,F) \cdot dF \tag{3}$$

In eq.(3) it has been assumed that Θ of the telescope orientation and Θ_{source} of the source direction are identical. In the case the two are different there is an additional dependence of $R^\gamma(E,\Theta,F)$ and

$F^{\gamma}_{eff}(E,\Theta)$ on Θ_{source}. However, often Θ and Θ_{source} are very close, in which case their difference can be ignored.

A side remark : The well known behaviour that the effective collection area (well above the threshold energy) is larger for larger zenith angles Θ, is due to the fact that at higher Θ the distance of the shower maximum (where the majority of Cherenkov photons is emitted) from the detector is larger than at smaller Θ. The area in which $R^{\gamma}(E,\Theta,F)$ contributes significantly to the integral (3) is therefore larger, resulting in a larger $F^{\gamma}_{eff}(E,\Theta)$. For the simulation this means, that the maximum impact parameter p_{max} has to be chosen larger for larger Θ. A rough estimate suggests $p_{max}(\Theta) \;=\; f(\Theta)\cdot p_{max}(20^\circ)$ with $f(\Theta) \;=\; 1.3,\ 1.6,\ 1.9,\ 2.8,\ 5.4,\ 21.5$ for $\Theta \;=\; 40^\circ,\ 50^\circ,\ 60^\circ,\ 70^\circ,\ 80^\circ,\ 90^\circ$ respectively.

For infinitesimal $dE,\ dF,\ dt$ the number of 'observed' γs is

$$dN_s^{\gamma,obs}(E,\Theta,F) \;=\; \Phi_s^{\gamma}(E)\cdot R^{\gamma}(E,\Theta,F)\cdot dE\cdot dF\cdot dt \tag{4}$$

The number of γ showers observed in the bin $\Delta\Theta$ of the zenith angle and in the bin ΔE of the energy is then :

$$\begin{aligned}\Delta N_s^{\gamma,obs}(E,\Theta) \;&=\; \int \Phi_s^{\gamma}(E)\cdot R^{\gamma}(E,\Theta,F)\cdot dE\cdot dF\cdot dt &(5)\\ &=\; \Delta T_{on}(\Theta)\cdot \int_{\Delta E}\Phi_s^{\gamma}(E)\cdot F^{\gamma}_{eff}(E,\Theta)\cdot dE &(6)\end{aligned}$$

Here $\Delta T_{on}(\Theta)$ is the effective on-time for the data taken in the zenith angle bin $\Delta\Theta$. Assuming that $F^{\gamma}_{eff}(E,\Theta)$ depends only weakly on E in the (sufficiently small) interval ΔE gives

$$\begin{aligned}\Delta N_s^{\gamma,obs}(E,\Theta) \;&\approx\; \Delta T_{on}(\Theta)\cdot F^{\gamma}_{eff}(E,\Theta)\cdot \int_{\Delta E}\Phi_s^{\gamma}(E)\cdot dE &(7)\\ &\approx\; \Delta T_{on}(\Theta)\cdot F^{\gamma}_{eff}(E,\Theta)\cdot \Delta E\cdot \overline{\Phi_s^{\gamma}}(E) &(8)\end{aligned}$$

where $\overline{\Phi_s^{\gamma}}(E)$ is the average differential gamma flux in the energy bin ΔE :

$$\overline{\Phi_s^{\gamma}}(E) \;=\; \frac{1}{\Delta E}\int_{\Delta E}\Phi_s^{\gamma}(E)\cdot dE \tag{9}$$

In the same approximation the number of true γs is obtained from (8) by setting $F^{\gamma}_{eff}(E,\Theta) \;=\; \Delta F$, where ΔF may be any area which is of interest :

$$\Delta N_s^{\gamma,true}(E,\Theta) \;\approx\; \Delta T_{on}(\Theta)\cdot\Delta F\cdot\Delta E\cdot\overline{\Phi_s^{\gamma}}(E) \tag{10}$$

By inverting equation (8) and setting $\Delta E \;=\; (E^{up}-E^{low})$ the average flux $\overline{\Phi_s^{\gamma}}(E)$ can be written as

$$\overline{\Phi_s^{\gamma}}(E) \;=\; \frac{\Delta N_s^{\gamma,obs}(E,\Theta)}{\Delta T_{on}(\Theta)\cdot F^{\gamma}_{eff}(E,\Theta)}\cdot\frac{1}{(E^{up}-E^{low})} \tag{11}$$

By means of equation (11) $\overline{\Phi_s^\gamma}(E)$ can be determined from the measured $\Delta N_s^{\gamma,obs}(E,\Theta)$ and $\Delta T_{on}(\Theta)$, using the effective collection area $F_{eff}^\gamma(E,\Theta)$, which is obtained from MC data (see b)). If everything was done correctly the result for $\overline{\Phi_s^\gamma}(E)$ should be independent of the Θ range in which data were taken.

Equation (11) is for a limited and fixed region of the zenith angle. One may calculate $\overline{\Phi_s^\gamma}(E)$ from the data taken at all Θ, in which case

$$\overline{\Phi_s^\gamma}(E) = \frac{\sum_i \Delta N_s^{\gamma,obs}(E,\Theta_i)}{\sum_i \Delta T_{on}(\Theta_i)\cdot F_{eff}^\gamma(E,\Theta_i)} \cdot \frac{1}{(E^{up}-E^{low})} \tag{12}$$

If a fixed spectral index α is assumed for the differential source spectrum

$$\Phi_s^\gamma(E) = \Phi_0^\gamma \cdot \left(\frac{E}{GeV}\right)^{-\alpha} \tag{13}$$

one gets

$$\int_{\Delta E} \Phi_s^\gamma(E)\cdot dE = \frac{\Phi_0^\gamma}{1-\alpha}\left[\left(\frac{E^{up}}{GeV}\right)^{1-\alpha} - \left(\frac{E^{low}}{GeV}\right)^{1-\alpha}\right]\cdot GeV = (E^{up}-E^{low})\cdot\overline{\Phi_s^\gamma}(E) \tag{14}$$

Inserting (14) into (11) yields

$$\Phi_0^\gamma = \frac{\Delta N_s^{\gamma,obs}(E,\Theta)}{\Delta T_{on}(\Theta)\cdot F_{eff}^\gamma(E,\Theta)} \cdot \frac{1}{\left[\left(\frac{E^{up}}{GeV}\right)^{1-\alpha} - \left(\frac{E^{low}}{GeV}\right)^{1-\alpha}\right]} \cdot \frac{1-\alpha}{GeV} \tag{15}$$

which by summing over all Θ bins gives

$$\Phi_0^\gamma = \frac{\sum_i \Delta N_s^{\gamma,obs}(E,\Theta_i)}{\sum_i \Delta T_{on}(\Theta_i)\cdot F_{eff}^\gamma(E,\Theta_i)} \cdot \frac{1}{\left[\left(\frac{E^{up}}{GeV}\right)^{1-\alpha} - \left(\frac{E^{low}}{GeV}\right)^{1-\alpha}\right]} \cdot \frac{1-\alpha}{GeV} \tag{16}$$

b) Effective collection area for point sources

If the above formulas are applied to MC data $R^\gamma(E,\Theta,F)$ can be obtained from (2) and (4) as

$$R^\gamma(E,\Theta,F) = \frac{\Delta N_s^{\gamma,MC,obs}(E,\Theta,F)}{\Delta N_s^{\gamma,MC,generated}(E,\Theta,F)} \tag{17}$$

Using (8) and (10) the effective collection area can be determined as

$$F^{\gamma}_{eff}(E,\Theta) \;=\; \frac{\Delta N_s^{\gamma,MC,obs}(E,\Theta)}{\Delta N_s^{\gamma,MC,generated}(E,\Theta)} \cdot \Delta F(\Theta_{source}) \tag{18}$$

In (18) $\Delta F(\Theta_{source})$ is the size of the area (perpendicular to the source direction) in which MC events were generated. If the events were generated in a horizontal plane of size $F_{horizontal}$ and the source is at a zenith angle Θ_{source}, $\Delta F(\Theta_{source})$ is equal to $F_{horizontal} \cdot \cos\Theta_{source}$. Note that Θ and Θ_{source} need not be identical.

Using (18) for determining F^{γ}_{eff} is of course simpler than calculating R^{γ} via (17) and performing the integration (3). This procedure of determining $F^{\gamma}_{eff}(E,\Theta)$ amounts to performing the integration in equation (3) by MC. An important precondition is that in the MC simulation all gamma showers for which $R^{\gamma}(E,\Theta,F)$ is greater than zero were simulated. This means in particular that the MC simulation of gammas extends to sufficiently large impact parameters, i.e. to sufficiently large $\Delta F(\Theta_{source})$. In practice, in order to save computer time, showers will be generated up to a maximum value of the impact parameter p_{max} (see Section 3.2 a)). A suitable correction for that has to be applied later in the analysis.

Knowing $F^{\gamma}_{eff}(E,\Theta)$, the gamma fluxes can be obtained from the experimental data using equation (11), (12), (15) or (16).

Of course, the MC data sample used for calculating $F^{\gamma}_{eff}(E,\Theta)$ and the experimental data sample used for determining the gamma flux by means of $F^{\gamma}_{eff}(E,\Theta)$ have to be defined identically in many respects : in particular the set of cuts and the offset between source position and telescope orientation have to be the same in the MC data and the experimental data sample.

c) Differential flux of hadronic cosmic rays

In the case of hadronic cosmic rays, which arrive from all directions Ω, the differential hadron flux is given by

$$\Phi^h(E) \;=\; \frac{dN^h}{dE \cdot dF \cdot dt \cdot d\Omega} \tag{19}$$

In contrast to (3) the effective collection area for hadrons is defined as

$$F^{h}_{eff}(E,\Theta) \;=\; \int R^h(E,\Theta,F,\Omega) \cdot dF \cdot d\Omega \tag{20}$$

Note that for a fixed orientation of the telescope (Θ,ϕ) the hadrons are coming from all directions Ω. The reconstruction efficiency $R^h(E,\Theta,F,\Omega)$ of hadrons therefore depends also on Ω.

With the definitions (19) and (20) very similar formulas are obtained for hadrons as were derived for photons in the previous sections. For clarity they are written down explicitely :

For infinitesimal dE, dF, dt, $d\Omega$ the number of true hadrons is

$$dN^{h,true}(E,\Theta,F,\Omega) \;=\; \Phi^h(E)\cdot dE\cdot dF\cdot dt\cdot d\Omega \tag{21}$$

and the number of 'observed' hadrons

$$dN^{h,obs}(E,\Theta,F,\Omega) \;=\; \Phi^h(E)\cdot R^h(E,\Theta,F,\Omega)\cdot dE\cdot dF\cdot dt\cdot d\Omega \tag{22}$$

Integrating over dF and $d\Omega$ yields

$$\begin{aligned} \Delta N^{h,obs}(E,\Theta) &= \int \Phi^h(E)\cdot R^h(E,\Theta,F,\Omega)\cdot dE\cdot dF\cdot dt\cdot d\Omega & (23)\\ &= \Delta T_{on}(\Theta)\cdot\int_{\Delta E}\Phi^h(E)\cdot F^h_{eff}(E,\Theta)\cdot dE & (24) \end{aligned}$$

$$\begin{aligned} \Delta N^{h,obs}(E,\Theta) &\approx \Delta T_{on}(\Theta)\cdot F^h_{eff}(E,\Theta)\cdot\int_{\Delta E}\Phi^h(E)\cdot dE & (25)\\ &\approx \Delta T_{on}(\Theta)\cdot F^h_{eff}(E,\Theta)\cdot\Delta E\cdot\overline{\Phi^h}(E) & (26) \end{aligned}$$

with

$$\overline{\Phi^h}(E) \;=\; \frac{1}{\Delta E}\int_{\Delta E}\Phi^h(E)\cdot dE \tag{27}$$

In the same approximation the number of true hadrons is obtained from (26) by setting $F^h_{eff}(E,\Theta) = \Delta F\cdot\Delta\Omega$, where ΔF and $\Delta\Omega$ may be any area or angular range which is of interest :

$$\Delta N^{h,true}(E,\Theta) \;\approx\; \Delta T_{on}(\Theta)\cdot\Delta F\cdot\Delta\Omega\cdot\Delta E\cdot\overline{\Phi^h}(E) \tag{28}$$

Using (26) and setting $\Delta E \;=\; (E^{up}-E^{low})$ one obtains

$$\overline{\Phi^h}(E) \;=\; \frac{\Delta N^{h,obs}(E,\Theta)}{\Delta T_{on}(\Theta)\cdot F^h_{eff}(E,\Theta)}\cdot\frac{1}{(E^{up}-E^{low})} \tag{29}$$

This relation can be used to determine $\overline{\Phi^h}(E)$ from the measured $\Delta N^{h,obs}(E,\Theta)$ and $\Delta T_{on}(\Theta)$, using the effective collection area $F^h_{eff}(E,\Theta)$, which is obtained from MC data (see d)). Again, the result for $\overline{\Phi^h}(E)$ should be independent of the Θ range in which data were taken. Summing over the different Θ intervals gives

$$\overline{\Phi^h}(E) \;=\; \frac{\sum_i\Delta N^{h,obs}(E,\Theta_i)}{\sum_i\Delta T_{on}(\Theta_i)\cdot F^h_{eff}(E,\Theta_i)}\cdot\frac{1}{(E^{up}-E^{low})} \tag{30}$$

If the differential hadron flux is parametrized as

$$\Phi^h(E) \;=\; \Phi^h_0 \cdot \left(\frac{E}{GeV}\right)^{-\beta} \tag{31}$$

the integrated hadron flux is

$$\int_{\Delta E} \Phi^h(E) \cdot dE \;=\; \frac{\Phi^h_0}{1-\beta} \left[\left(\frac{E^{up}}{GeV}\right)^{1-\beta} - \left(\frac{E^{low}}{GeV}\right)^{1-\beta} \right] \cdot GeV \;=\; (E^{up} - E^{low}) \cdot \overline{\Phi^h}(E) \tag{32}$$

Inserting (32) into (26) yields

$$\Phi^h_0 \;=\; \frac{\Delta N^{h,obs}(E,\Theta)}{\Delta T_{on}(\Theta) \cdot F^h_{eff}(E,\Theta)} \cdot \frac{1}{\left[\left(\frac{E^{up}}{GeV}\right)^{1-\beta} - \left(\frac{E^{low}}{GeV}\right)^{1-\beta} \right]} \cdot \frac{1-\beta}{GeV} \tag{33}$$

which by summing over all Θ bins gives

$$\Phi^h_0 \;=\; \frac{\sum_i \Delta N^{h,obs}(E,\Theta_i)}{\sum_i \Delta T_{on}(\Theta_i) \cdot F^h_{eff}(E,\Theta_i)} \cdot \frac{1}{\left[\left(\frac{E^{up}}{GeV}\right)^{1-\beta} - \left(\frac{E^{low}}{GeV}\right)^{1-\beta} \right]} \cdot \frac{1-\beta}{GeV} \tag{34}$$

Note that $\Phi^h(E)$, Φ^h_0 and $F^h_{eff}(E,\Theta)$ differ from $\Phi^\gamma(E)$, Φ^γ_0 and $F^\gamma_{eff}(E,\Theta)$ by the dimension of the solid angle, due to the additional factor $d\Omega$ in (19) and (20).

d) Effective collection area for hadronic cosmic rays

Applying (21) and (22) to MC data $R^h(E,\Theta,F,\Omega)$ can be written as

$$R^h(E,\Theta,F,\Omega) \;=\; \frac{\Delta N^{h,MC,obs}_s(E,\Theta,F,\Omega)}{\Delta N^{h,MC,generated}_s(E,\Theta,F,\Omega)} \tag{35}$$

Using (26) and (28) the expression for the effective collection area reads

$$F^h_{eff}(E,\Theta) \;=\; \frac{\Delta N^{h,MC,obs}_s(E,\Theta)}{\Delta N^{h,MC,generated}_s(E,\Theta)} \cdot \Delta F(\Theta) \cdot \Delta\Omega \tag{36}$$

Here $\Delta F(\Theta)$ is the size of the area (perpendicular to the direction of the telescope axis) in which MC events were generated. If the events were generated in a horizontal plane of size $F_{horizontal}$ and the zenith angle of the direction of the telescope is Θ, $\Delta F(\Theta)$ is equal to $F_{horizontal} \cdot \cos\Theta$. $\Delta\Omega$ is the size of the angular region (around the direction of the telescope axis) in which hadron showers were generated.

It goes without saying, that determining $F^h_{eff}(E,\Theta)$ according to (36) is simpler than calculating $R^h(E,\Theta,F,\Omega)$ via (35) and performing the integration (20).

This procedure of determining $F^h_{eff}(E,\Theta)$ amounts to performing the integrations in equation (20) by MC. The precondition in the case of hadrons is that in the MC simulation all hadron showers for which $R^h(E,\Theta,F,\Omega)$ is greater than zero were simulated. So the simulation should not only include large enough impact parameters (i.e. large $\Delta F(\Theta)$) but also a sufficiently large range of Ω (i.e. large $\Delta\Omega$) at fixed orientation (Θ,ϕ) of the telescope.

Knowing $F^h_{eff}(E,\Theta)$, the hadron fluxes can be obtained from the experimental data using equation (29), (30), (33) or (34).

e) Determining the absolute differential flux of gammas from a point source by normalizing to the flux of hadronic cosmic rays

In sections 3.2 a) and b) a procedure was described for measuring the absolute differential flux of gammas from a point source. The result for $\overline{\Phi^\gamma_s}(E)$ depends on the measurement of the on-time $\Delta T_{on}(\Theta)$ and on a reliable determination of the effective collection area $F^\gamma_{eff}(E,\Theta)$ by MC. A good MC simulation is therefore crucial.

The dependence on the MC simulation may be reduced by normalizing to the known differential flux of hadronic cosmic rays. Combining equations (11) and (29), and assuming that $\Delta T_{on}(\Theta)$ is the same for the gamma and the hadron sample, yields

$$\frac{\overline{\Phi^\gamma_s}(E)}{\overline{\Phi^h}(E)} = \frac{\Delta N^{\gamma,obs}(E,\Theta)}{\Delta N^{h,obs}(E,\Theta)} \cdot \frac{F^h_{eff}(E,\Theta)}{F^\gamma_{eff}(E,\Theta)} \tag{37}$$

If $\overline{\Phi^h}(E)$ is assumed to be known from other experiments, equation (37) allows to determine $\overline{\Phi^\gamma_s}(E)$ from the experimental number of gamma and hadron showers using the effective collection areas for gammas and hadrons from the MC. Since only the ratio of the effective collection areas enters the dependence on the MC simulation is reduced.

If data from all zenith angles are to be used the corresponding expression for $\overline{\Phi^\gamma_s}(E)$ is (see equations (12) and (30))

$$\frac{\overline{\Phi^\gamma_s}(E)}{\overline{\Phi^h}(E)} = \frac{\sum_i \Delta N^{\gamma,obs}(E,\Theta_i)}{\sum_i \Delta N^{h,obs}(E,\Theta_i)} \cdot \frac{\sum_i \Delta T_{on}(\Theta_i) \cdot F^h_{eff}(E,\Theta_i)}{\sum_i \Delta T_{on}(\Theta_i) \cdot F^\gamma_{eff}(E,\Theta_i)} \tag{38}$$

Clearly, the set of cuts defining the gamma sample is different from the set of cuts defining the hadron sample. However, $\Delta N^{\gamma,obs}$ and $\Delta N^{h,obs}$ can still be measured simultaneously, in which case $\Delta T_{on}(\Theta_i)$ is the same for the gamma and the hadron sample. Measuring gammas and hadrons simultaneously has the advantage that variations of the detector properties or of the atmospheric conditions during the observation partly cancel in (37) and (38).

If fixed spectral indices α and β are assumed for the differential gamma and the hadron fluxes respectively one obtains for the ratio $\Phi^\gamma_0 \ / \ \Phi^h_0$ (see (15) and (33))

$$\frac{\Phi_0^\gamma}{\Phi_0^h} = \frac{\Delta N^{\gamma,obs}(E,\Theta)}{\Delta N^{h,obs}(E,\Theta)} \cdot \frac{F_{eff}^h(E,\Theta)}{F_{eff}^\gamma(E,\Theta)} \cdot \frac{\left[\left(\frac{E^{up}}{GeV}\right)^{1-\beta} - \left(\frac{E^{low}}{GeV}\right)^{1-\beta}\right]}{\left[\left(\frac{E^{up}}{GeV}\right)^{1-\alpha} - \left(\frac{E^{low}}{GeV}\right)^{1-\alpha}\right]} \cdot \frac{1-\alpha}{1-\beta} \tag{39}$$

or, when using the data from all zenith angles, (see (16) and (34))

$$\frac{\Phi_0^\gamma}{\Phi_0^h} = \frac{\sum_i \Delta N^{\gamma,obs}(E,\Theta_i)}{\sum_i \Delta N^{h,obs}(E,\Theta_i)} \cdot \frac{\sum_i \Delta T_{on}(\Theta_i) \cdot F_{eff}^h(E,\Theta_i)}{\sum_i \Delta T_{on}(\Theta_i) \cdot F_{eff}^\gamma(E,\Theta_i)} \cdot \frac{\left[\left(\frac{E^{up}}{GeV}\right)^{1-\beta} - \left(\frac{E^{low}}{GeV}\right)^{1-\beta}\right]}{\left[\left(\frac{E^{up}}{GeV}\right)^{1-\alpha} - \left(\frac{E^{low}}{GeV}\right)^{1-\alpha}\right]} \cdot \frac{1-\alpha}{1-\beta} \tag{40}$$

The normalization to the known flux of hadronic cosmic rays can of course only be done if the MC simulation includes the simulation of all hadrons (protons, He, and higher elements), with the right chemical composition and energy spectra. In addition, the background from diffuse electrons has to be taken into account (see [10]).

4 MC work

4.1 Overview of the MC simulation and analysis chain

Due to the big amount of diskspace needed for MC simulation it was decided to split up the simulation into various substeps. Figure 1 gives an overview of the existing programs and the connections between them. A description of the different programs can be found in section 4.2. From the diagram in Fig. 1 one can see the following features of the simulation and analysis chain of MAGIC.

- The simulation of air showers (done in MMCS) and the simulation of the night sky background (NSB) are separated.
- The mirror dish and the response of all MAGIC mirrors to the Cherenkov photons from the showers are simulated in the *reflector* program.
- The NSB contribution is separated into two parts, the contribution from the starfield and that from the diffuse background.
- To speed up the production the starresponse program creates a database for stars of different magnitudes.
- The merging of air showers and the NSB is done in the *camera* program.
- The reconstruction and analysis of MC and real data is done by the same program. This program is called MARS (MAGIC Analysis and Reconstruction Software). The format of the output of the *camera* program for MC data is identical to the format of the output of the MERPP (MERging and PreProcessing) program for the real data. The output files are written in the ROOT format.

In the next section the usage of the Monte Carlo programs is explained. The description of the MERPP and MARS programs can be found elsewhere ([8]).

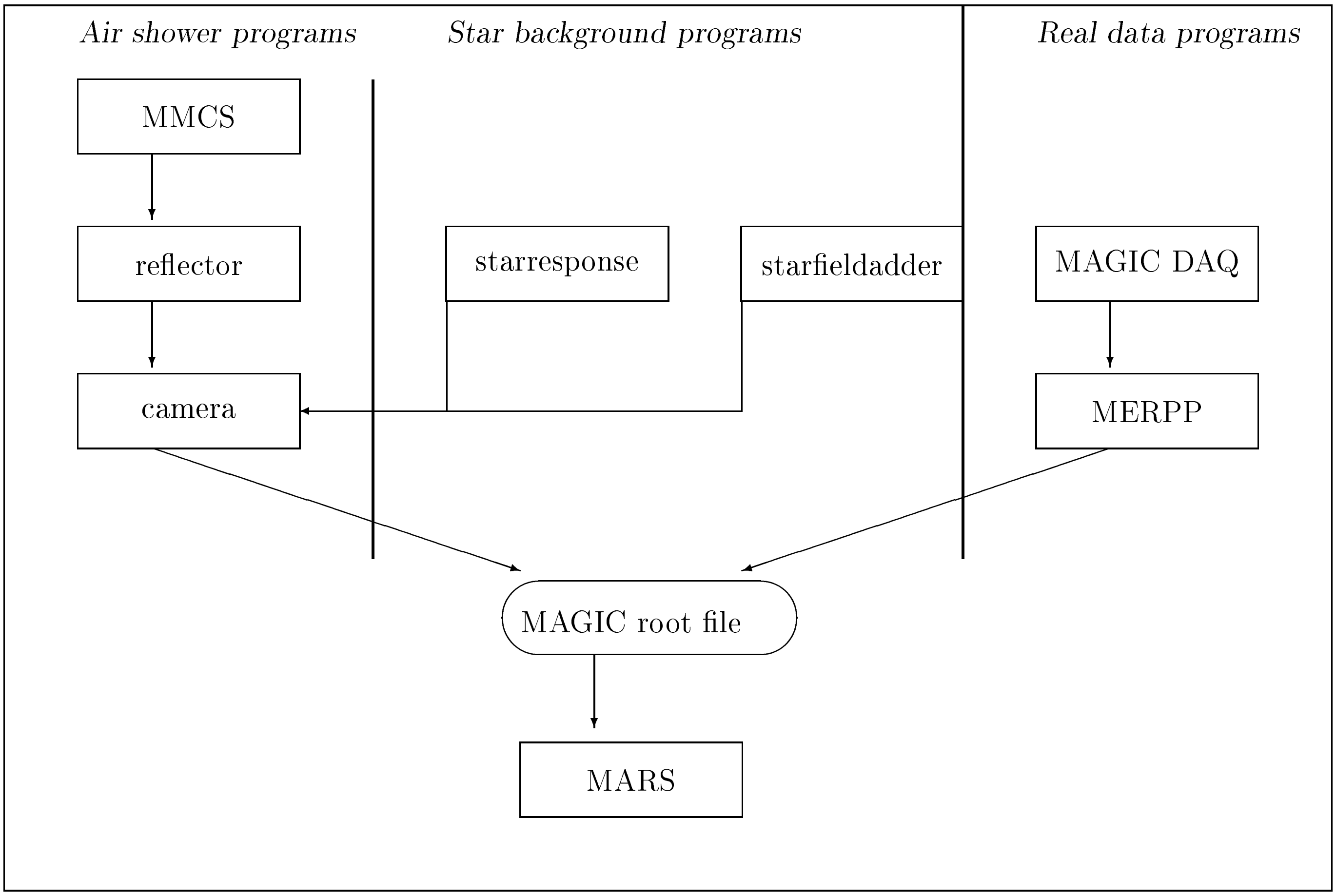

Figure 1: Overview of the existing programs in the MC of MAGIC.

4.2 Existing programs

Some information on the MC programs can found on the web under the address given in [9] ==¿ User guide.

4.2.1 MMCS - MAGIC Monte Carlo Simulation

This program is based on a CORSIKA simulation. It generates air showers for the MAGIC telescope. At the start of a run of the program, one has to define several parameters for the simulation (see also figure 2):

- The type of the particle ($PartID$)
- The energy range (E_1, E_2)
- The spectral index of the differential energy spectrum
- The radius r_{Core} ($\sim$ 300 m at low Θ) of a circular region on the ground around the telescope position for the shower core positions
- The radius r_{photon} ($\sim$ 20 m) of a sphere around the telescope for the Cherenkov photons to be kept

- The ranges (Θ_1, Θ_2) and (ϕ_1, ϕ_2) of the zenith and azimuthal angles (Θ_{CR}, ϕ_{CR}) of the cosmic ray particle direction

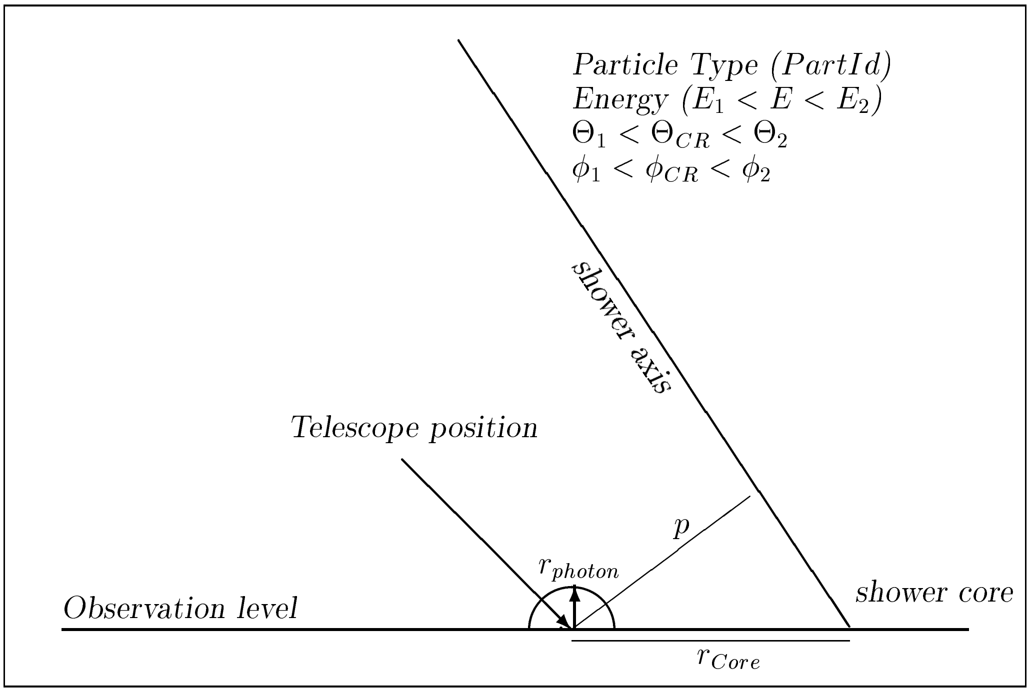

Figure 2: The parameters of a cosmic ray particle to be specified at the beginning of a MMCS run, and the definition of the impact parameter p.

The program MMCS tracks the whole shower development through the atmosphere. After the shower core position on the ground has been chosen, all Cherenkov photons hitting the sphere with radius r_{photon} around the telescope are stored on disk. These Cherenkov photons are the input for the next program, called *reflector*. It is important to note, that up to now the telescope orientation has not been used.

Other parameters, that will be important in the analysis later, are calculated. The impact parameter p, for example, is calculated from the direction of the shower (Θ_{CR}, ϕ_{CR}) and the core position (x_{core}, y_{core}). The penetration depth X_{max}, defined as the column density in the atmosphere at which the number of shower particles is maximum, should also be stored.

4.2.2 reflector

The aim of the *reflector* program is the tracking of the Cherenkov photons to the camera of the MAGIC telescope. This is the point where the orientation of the telescope (Θ, ϕ) enters. For all Cherenkov photons the program tests if the mirrors are hit, calculates the probability for the reflection and tracks the reflected photons to the mirror plane. All photons hitting the camera are written to disk (*.rfl), with the parameters (x_{camera}, y_{camera}) (= position in the camera), λ (wavelength of the photon) and $t_{arrival}$ (arrival time of the photon).

4.2.3 starfieldadder

This program simulates the starfield (the non-diffusive part of the night sky background) around a given source. This starfield depends on the wobble position. Note that the sky region projected onto the camera changes continuously when the offset $\Delta\beta$ is chosen to be an offset in local coordinates or in coordinates in the camera system [13].

The $starfieldadder$ program generates a CORSIKA like file containing those photons from the stars which reach the telescope. This file is processed by the $reflector$ program (with the atmospheric absorption switched off), which produces the files which are then input to the $camera$ program.

4.2.4 starresponse

This program simulates the night sky background response. It simulates a) the analog signal, which together with the shower contribution will go to the trigger discriminator, and b) the FADC signal for a given number of photo electrons per ns, coming from the stars and/or the diffuse night sky background. Actually it generates these signals for a much longer time than that used for each simulated shower, creating a database. The $camera$ program will read only the needed time interval, choosing the starting point randomly.

4.2.5 camera

Instructions for running the $camera$ program are given in [11].

The input to the $camera$ program are the parameters $(x_{camera},\ y_{camera})$, λ and $t_{arrival}$ from the $reflector$ program, as well as the data from the *starresponse* and $starfieldadder$ programs.

The *camera* program simulates the behaviour of the PMTs and the electronics of the trigger and FADC system. For each photon in the reflector file (*.rfl) the *camera* program calculates the probability to generate a photoelectron in the photocathode. If a photoelectron was ejected, it will create a signal in the trigger and FADC system of the respective pixel.

Before running *camera* one has to specify the parameters of the signal shaping (shape, amplitude, FWHM of signal), separatly for the trigger and the FADC system.

For each pixel, the signals from all photoelectrons are superimposed. All these analog signals go into the trigger system.

At the start of the *camera* program one has to set a few parameters for the trigger system, like:

- Discriminator threshold
- Mulitplicity of triggering pixels
- Coincidence time interval
- Topology of pixels

With this set of parameters the *camera* program will check whether the event has triggered. For the triggered events all the FADC content will be written onto the file '*.root'. In addition all the information about the event $(PartID, E, \Theta_{CR},...)$ and the trigger information (FirstLevel, SecondLevel, ..) are also written onto the file.

4.3 MC event generation and MC studies

One of the aims of this report is to give a complete list of things to be done in order to be able to determine photon fluxes from point sources. To be explicit, the list is given for the Crab nebula, which we propose to start with.

a) The event generation for the Crab should be done with the following conditions:

- Range of Θ_{CR} : $0 < \Theta_{CR} < 25°$ (for the time being)
- Statistics : at least 20 000 triggers
- Mode of observation : wobble mode as proposed in Section 2.1
- Adapt *starfieldadder* and *starresponse* to the Crab; assume a fixed star field (no rotation and no change with time) in the field of view of the camera, for the time being
- Pedestal fluctuations: for each pixel, the amplitude (in terms of photoelectrons) is smeared according to a Poissonian with a mean of 1.5 photo electrons
- Trigger: see Section 2.4

b) Using these data and the data from the simulation of the diffuse background from electrons and hadrons the following tasks have to be performed with the MARS program :

- Define the γ/(hadron+electron) separation in terms of cuts on image parameters, as a function of Θ and the pedestal fluctuations (later also as a function of the PM-HV settings)
- Define *standard cuts* for γ and hadron samples
- Determine the effective collection areas (see Sections 3b) and 3d)) for γs and hadrons (for the *standard cuts*), as a function of Θ and the pedestal fluctuations (later also as a function of the PM-HV settings)
- Find estimators E^{γ}_{est} and E^{h}_{est} for the true energy E of photon and hadron showers respectively
- Determine the migration matrices (E, E^{γ}_{est}) and (E, E^{h}_{est}) as a function of Θ and the pedestal fluctuations (later also as a function of the PM-HV settings). The migration matrices are needed for the unfolding of the experimental distributions of E^{γ}_{est} and E^{h}_{est} to obtain the distributions of the true energy E.

c) Of general interest will also be :

- The energy threshold as a function of Θ and the pedestal fluctuations (later also as a function of the PM-HV settings). The energy threshold is usually defined as the energy where the effective collection area reaches 50 % of its maximum value, or as the energy where the differential energy spectrum $\mathrm{d}N_{reconstructed}/\mathrm{d}E$ of reconstructed events has its maximum, or as the energy E_0 for which the integrated flux $\frac{\mathrm{d}N}{\mathrm{d}F \cdot \mathrm{d}t}(E > E_0)$ (which is known from other experiments) is equal to the integrated observed flux (not corrected for trigger losses). The first definition is preferred because it is independent of the energy spectrum. Of course, the energy threshold can be calculated at different levels : after the trigger, after reconstruction, after the *standard cuts*, etc. . For first studies see [14].
- The sensitivity of MAGIC as a function of Θ and the pedestal fluctuations (later also as a function of the PM-HV settings). The sensitivity is defined as the minimum photon flux that can be measured with 5 sigmas within 50 hours of observation time

- The trigger rate for MAGIC as a function of Θ and the pedestal fluctuations (later also as a function of the PM-HV settings). For first studies see [14].
- The angular and energy resolution as a function of Θ and the pedestal fluctuations (later also as a function of the PM-HV settings).
- Checks of the absolute flux and energy scale. Such checks can for example be made by comparing absolute fluxes as determined from experimental data taken with MAGIC (using the number of observed showers, the effective collection area and the on-time) with the fluxes as measured by other experiments.

For some results from first studies see [12].

d) Additional studies should be made on :

- the influence of the geomagnetic field (see [10])
- effects due to the rotating (see [5]) and changing star field in the camera
- the reconstruction efficiency R^γ for photon showers (see Section 3b)) as a function of the impact parameter, and the reconstruction efficiency R^h for hadron showers (see Section 3d)) as a function of the impact parameter and of Ω.

5 Analysis of the real data

The set of tasks to be performed for determining absolute fluxes of point sources is subdivided into the tasks dealing with pixels (Section 5.1), those dealing with events (Section 5.2) and those dealing with final calculations (Section 5.3). In general (but not always) each task will correspond to a task in the sense of C++. These tasks should exist and be tested on Monte Carlo data before the first observations from MAGIC become available.

5.1 Tasks concerning individual pixels

a) From pedestal events

- Calculate the average pedestal P and the pedestal fluctuation σ_P and their errors $\Delta P, \Delta\sigma_P$, for low and high gain
- Do the correction for coherent electronic pickup
- Give the range of validity (in absolute time) for the current P, σ_P

b) From light calibration events

- Determine the conversion factor $\int$FADC $\longleftrightarrow N_\gamma$ (number of photons), for low and high gain
- Determine the relative time calibration between the pixels

c) For physics triggered events. For each pixel

- Subtract the pedestals

- Calculate $\int$FADC for low and high gain
- Convert $\int$FADC into N_γ
- Determine the relative arrival time $\tilde{t}$ of the photon bunch
- Store N_γ, ΔN_γ and $\tilde{t}$

5.2 Tasks concerning all pixels together

a) From oscillation monitor events
Determine the current camera coordinate system, i.e. the shifts $\Delta x, \Delta y$ and the rotation angle $\Delta\epsilon$ relative to a standard camera coordinate system.

b) From the guiding system
Determine the position of the source and the orientation of star field in the camera.

c) From the GPS
Get the absolute time.

d) For physics triggered events :

- Check whether the event has triggered
- Determine the number of islands and mountains using N_γ, ΔN_γ, $\tilde{t}$, σ_P for each pixel.
- Do image cleaning using N_γ, ΔN_γ, $\tilde{t}$, σ_P for each pixel.
- Determine the image parameters and their errors. The parameters MISS, DIST and ALPHA have to be calculated for both the source position and for the 'anti' source position in the camera. Parameters have to be introduced which describe the *time* structure of the image.
- Calculate the estimators E^γ_{est} and E^h_{est} of the shower energy from the image parameters, Θ and the pedestal fluctuations.
- Determine the absolute time t of the event
- Fill histograms :
  - The image parameters for different bins of (E^γ_{est}, t), for the source and the 'anti' source position in the camera
  - The image parameters for different bins of (E^h_{est}, t), for the 'anti' source position
  - The time difference Δt between subsequent events for different bins of t (needed for the calculation of the effective on-time)

5.3 Tasks concerning final calculations

- Determine the effective on-time for the different bins of t
- For photons :

- Determine N_γ as a function of (E^γ_{est}, t) from the ALPHA distributions for the source and the 'anti' source position $\Longrightarrow \dfrac{\mathrm{d}N^{rec}_\gamma}{\mathrm{d}E^\gamma_{est}}\,(E^\gamma_{est}, t)$
- Unfold $\dfrac{\mathrm{d}N^{rec}_\gamma}{\mathrm{d}E^\gamma_{est}}\,(E^\gamma_{est}, t)$ to get $\dfrac{\mathrm{d}N^{rec}_\gamma}{\mathrm{d}E}\,(E, t)$
- Convert $\dfrac{\mathrm{d}N^{rec}_\gamma}{\mathrm{d}E}\,(E, t)$ into the absolute fluxes $\dfrac{\mathrm{d}N_\gamma}{\mathrm{d}E \cdot \mathrm{d}F \cdot \mathrm{d}t}\,(E, t)$ using the effective collection areas (from MC) and the effective on-time
- Plot as a function of the time :
  * number of events in the signal region
  * number of background events in the signal region
  * number of signal events (and its error) in the signal region
  * significance
  * signal/background ratio (and its error)
- Plot the light curve $\dfrac{\mathrm{d}N_\gamma}{\mathrm{d}F \cdot \mathrm{d}t}\,(t)$
- Plot the energy distribution $\dfrac{\mathrm{d}N_\gamma}{\mathrm{d}E \cdot \mathrm{d}F \cdot \mathrm{d}t}\,(E)$

• For hadrons :

- Determine N_h as a function of $(E^h_{est}, t) \Longrightarrow \dfrac{\mathrm{d}N^{rec}_h}{\mathrm{d}E^h_{est}}\,(E^h_{est}, t)$
- Unfold $\dfrac{\mathrm{d}N^{rec}_h}{\mathrm{d}E^h_{est}}\,(E^h_{est}, t)$ to get $\dfrac{\mathrm{d}N^{rec}_h}{\mathrm{d}E}\,(E, t)$
- Convert $\dfrac{\mathrm{d}N^{rec}_h}{\mathrm{d}E}\,(E, t)$ into the absolute fluxes $\dfrac{\mathrm{d}N_h}{\mathrm{d}E \cdot \mathrm{d}F \cdot \mathrm{d}\Omega \cdot \mathrm{d}t}\,(E, t)$ using the effective collection areas (from MC) and the effective on-time
- Plot the light curve $\dfrac{\mathrm{d}N_h}{\mathrm{d}F \cdot \mathrm{d}\Omega \cdot \mathrm{d}t}\,(t)$
- Plot the energy distribution $\dfrac{\mathrm{d}N_h}{\mathrm{d}E \cdot \mathrm{d}F \cdot \mathrm{d}\Omega \cdot \mathrm{d}t}\,(E)$

References

[1] A.M. Hillas, Proc. 19th ICRC, La Jolla 3 (1985) 445

[2] P.T. Reynolds et al., ApJ 404 (1993) 206

[3] D.J. Fegan, Space Sci.Rev. 75 (1996)137

[4] A. Konopelko et al., Astropart. Phys. 10 (1999) 275

[5] W. Wittek, MAGIC-TDAS 00-11, 000727/WWittek (2000)

[6] D. Bastieri et al., MAGIC-TDAS 00-12, 000520/DBastieri (2000)

[7] J. Cortina, MAGIC-TDAS 01-02/1, 010426/JCortina (2001)

[8] http://hegra1.mppmu.mpg.de/MAGIC/private/software/

[9] http://hegra1.mppmu.mpg.de/MAGIC/private/montecarlo/

[10] J. Cortina, J.C. González, Astropart. Phys. 15 (2001) 203

[11] O. Blanch, MAGIC-TDAS 01-04, 010419/OBlanch (2001)

[12] O. Blanch et al., Proc. of the 27th ICRC at Hamburg, Vol. 7, 2931 (2001)

[13] W. Wittek, MAGIC-TDAS 01-05, 010830/WWittek (2001)

[14] O. Blanch, MAGIC-TDAS 01-xx, 010827/OBlanch (2001)